

# Cholesterols Induced Distinctive Entry of the Graphene Nanosheet into the Cell Membrane

Binbin Tan, Juanmei Hu,\* and Fengmin Wu\*

Cite This: *ACS Omega* 2024, 9, 9216–9225

Read Online

ACCESS |



Metrics &amp; More

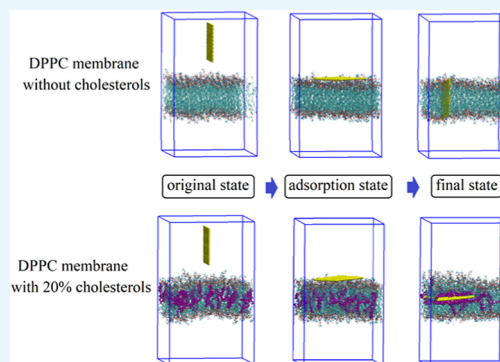


Article Recommendations



Supporting Information

**ABSTRACT:** Graphene nanosheets are highly valued in the biomedical field due to their potential applications in drug delivery, biological imaging, and biosensors. Their biological effects on mammalian cells may be influenced by cholesterols, which are crucial components in cell membranes that take part in many vital processes. Therefore, it is particularly important to investigate the effect of cholesterols on the transport mechanism of graphene nanosheets in the cell membrane as well as the final stable configuration of graphene, which may have an impact on cytotoxicity. In this paper, the molecular details of a graphene nanosheet interacting with a 1,2-dipalmitoyl-*sn*-glycero-3-phosphorylcholine (DPPC) membrane with cholesterols were studied using molecular dynamics simulations. Results showed that the structure of the graphene nanosheet transits from the cut-in state in a pure DPPC membrane to being sandwiched between two DPPC leaflets when cholesterols reach a certain concentration. The underlying mechanism showed that cholesterols are preferentially adsorbed on the graphene nanosheet, which causes a larger disturbance to the nearby DPPC tails and thus guides the graphene nanosheet into the core of lipid bilayers to form a sandwiched structure. Our results are helpful for understanding the fundamental interaction mechanism between the graphene nanosheet and cell membrane and to explore the potential applications of the graphene nanosheet in biomedical sciences.



## INTRODUCTION

The rapid development of nanomaterials in biological applications, such as therapeutics and diagnostics, requires a systematic understanding of bionano interactions urgently.<sup>1–3</sup> Bionano interactions are fundamental factors for cellular biological functions or potential cytotoxicity, which first occur at the cell plasma membrane. Studies have shown that the interaction between nanomaterials and the cell membrane is a complex process that can be influenced by many factors, such as the geometric shape and surface chemistry of nanomaterials,<sup>4</sup> the composition of cell membranes,<sup>5</sup> and the environment.<sup>6</sup> In general, attention is paid to the interaction mode, the steady configuration, and their effects on cell functions.

Cholesterols, which are multifunctional lipids unique to the eukaryotic membrane, are distributed in various tissues with amounts varying from approximately 20 to 50%.<sup>7</sup> The rigid steroid ring structure of cholesterol restricts the motion of other membrane lipid tails, which thereby modulates biophysical properties of mammalian plasma membranes,<sup>8</sup> such as membrane thickness,<sup>9</sup> fluidity,<sup>10,11</sup> and flexibility.<sup>12,13</sup> Despite the role of cholesterols in biosystems having been reported by a large amount of literature studies,<sup>14,15</sup> much remains unknown about the exact roles of cholesterols and their molecular interactions on the membrane function.<sup>16,17</sup> Based on their effect on the membrane permeability and molecular transport ability, Canepa et al. reported that the

passive uptake of amphiphilic nanoparticles into fluid lipid membranes can be significantly hindered by cholesterols.<sup>18</sup> Lorents et al. found that cholesterol-poor subdomains are favorable for the translocation of the arginine-rich cell-penetrating peptides across the cell membrane.<sup>19,20</sup> Moreover, cholesterol inhibition has molecular selectivity. Cholesterols restrains the uptake of THP but does not influence the uptake of EPT.<sup>21</sup> In tumor therapy, cholesterols contribute to the tumor adaptive response upon targeted mitogen-activated protein kinase pathway inhibitors.<sup>22</sup> Thus, the specific influence of cholesterols on the function of the cell membrane is complicated and should be analyzed case by case.

Graphene nanosheets have become promising candidates in biotechnology and biomedicine fields, such as drug delivery,<sup>23,24</sup> bioimaging, and antimicrobial and photothermal therapy of tumor or infection.<sup>25,26</sup> At the same time, biosafety of carbon nanomaterials is also an issue that cannot be ignored.<sup>27</sup> Potential toxicity may come from the disturbance to the cell membrane and their hybrid structure, as well as other

Received: October 19, 2023

Revised: January 19, 2024

Accepted: January 29, 2024

Published: February 19, 2024



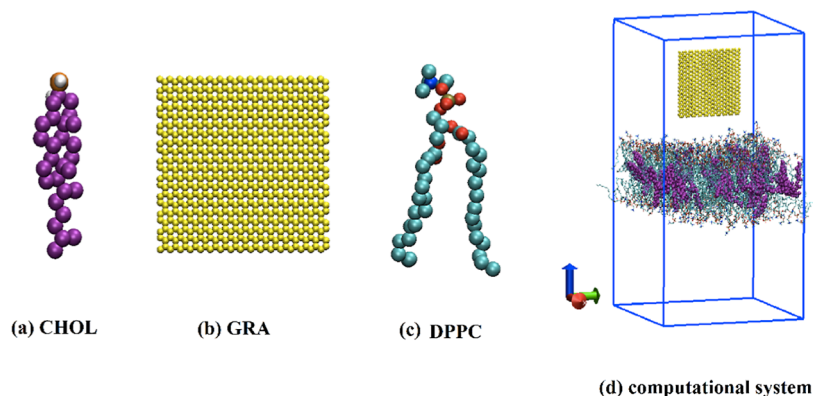


**Figure 1.** Molecular models of (a) cholesterol (CHOL), (b) pristine graphene nanosheet, and (c) DPPC. (d) The computational system is composed of a pristine graphene nanosheet and a membrane with DPPC lipids and cholesterols in a water environment. Water molecules are omitted for clarity. The graphene nanosheet was initially placed vertically above the membrane at a distance of 2 nm.

compositions that closely related to cellular functions.<sup>26</sup> Understanding the intricate interactions of graphene nanosheets on cell membranes is fundamental to determining their potential biomedical use as well as biocompatibility and cytotoxicity.

The hydrophobic properties and regular two-dimensional structure of graphene, combined with the rigid steroid ring structure of cholesterols, result in strong adsorption interactions between them.<sup>28,29</sup> Through the expressed physical interactions, graphene has been used to reduce the aggregation of cholesterols in the lysosome.<sup>30</sup> The activation of P<sub>2</sub>Y receptors has been promoted by an increase in cholesterols in fibroblasts grown on graphene. Based on these studies, the biological functions of the graphene nanosheets in the eukaryotic cell may be affected by cholesterols. For example, Kitko et al.<sup>31</sup> found that graphene increases cell membrane cholesterols and potentiates neurotransmission. Bernabo et al. found that graphene oxide is able to extract cholesterols from the spermatozoa membrane, which positively affects male gamete function.<sup>28</sup> These findings identify cholesterols as a mediator of graphene's cellular effects, but their exact role in driving graphene–membrane interactions remains controversial.

In this study, an atomistic molecular dynamics simulation was used to investigate the detailed dynamic process of graphene nanosheets into DPPC membranes with cholesterols and discuss the underlying molecular mechanism. It is found that the entry mode of the graphene nanosheet into the cell membrane will be impacted by cholesterols. Graphene nanosheets prefer to adopt parallel adsorption and then vertical insertion into pure DPPC bilayers or with low cholesterols. Contrarily, graphene nanosheets tend to obliquely insert into and, at last, be sandwiched between DPPC bilayers if the cholesterols reach a certain concentration. The intrinsic mechanism is discussed in detail below. These results indicate that in studying the biological function and potential toxicity of graphene nanosheets, the changes caused by cholesterol contents in different tissues should be considered.

## METHODOLOGY

Molecular dynamics simulation was used to verify the specific interactions of graphene nanosheets and the cell membrane in the presence of cholesterols. The cell membrane was assembled by 256 1,2-dipalmitoyl-*sn*-glycero-3-phosphorylcholine (DPPC)<sup>32</sup> and cholesterols, which were randomly

distributed in the DPPC bilayer with a mole percent from 0% to 30% with a GROMOS 54A7 force field.<sup>33,34</sup> The parameters of DPPC and cholesterols are from Berger's group.<sup>35</sup> The C–C bond of the graphene nanosheet is harmonic with an equilibrium length of 1.42 Å and a spring constant of  $4.00 \times 10^5$  kJ·mol<sup>-1</sup> nm<sup>-2</sup>. The balanced angles in graphene are set to 120° with a spring constant 600 kJ·mol<sup>-1</sup> rad<sup>-2</sup>, and the balanced dihedral of C–C–C–C is set to 180° with a spring constant of 3.00 kJ·mol<sup>-1</sup> rad<sup>-2</sup>. The carbon atoms in the graphene nanosheet are treated electrically neutral, and their Lennard-Jones parameters are  $\sigma_{cc} = 0.34$  nm and  $\epsilon_{cc} = 0.36$  kJ/mol.<sup>36</sup> The SPC model was used for water molecules.<sup>37</sup>

A simulation system with a size of 9.8 nm × 9.8 nm × 18 nm is hydrated by 14,000 water molecules with periodic boundary conditions, as shown in Figure 1. After 100 ns run, a graphene nanosheet was introduced to the aqueous phase vertically at a distance of 2 nm of the equilibrated membrane. Pristine graphene samples with the size of 3 nm × 3 nm, 4 nm × 4 nm, and 5 nm × 5 nm were used to test their interactions with the DPPC membrane.

All the simulations were taken at the *NPT* ensemble with a constant pressure of 1 atm and a constant temperature of 310 K. Using the Berendsen method, the pressures in *x* and *y* directions were coupled, while that in the *z* direction was controlled separately. The temperature of the cell membrane and other parts was controlled independently by a Berendsen thermostat. The electrostatic interactions were treated with the particle mesh Ewald method with the accuracy of  $1.0 \times 10^{-4}$ ,<sup>38</sup> and the van der Waals interaction with a Lennard-Jones potential was used with a cutoff distance at 12 Å. In each simulation, 300 ns was the total run time with a time step of 1 fs.<sup>39</sup> Simulation snapshots were obtained by using visual molecular dynamics software. All the simulations were performed using GROMACS 5.1.4 ([www.gromacs.org](http://www.gromacs.org)) package, and each condition was tested three times.

## RESULTS AND DISCUSSION

The dynamic interactions between a pristine graphene nanosheet with a size of 4 × 4 nm and a DPPC membrane without cholesterols were first investigated using molecular dynamics simulations. Figure 2a shows the temporal sequence during the interaction process, in which water molecules were omitted for clarity. Figure 2b shows the tilt angle of the graphene nanosheet and the corresponding distance of the

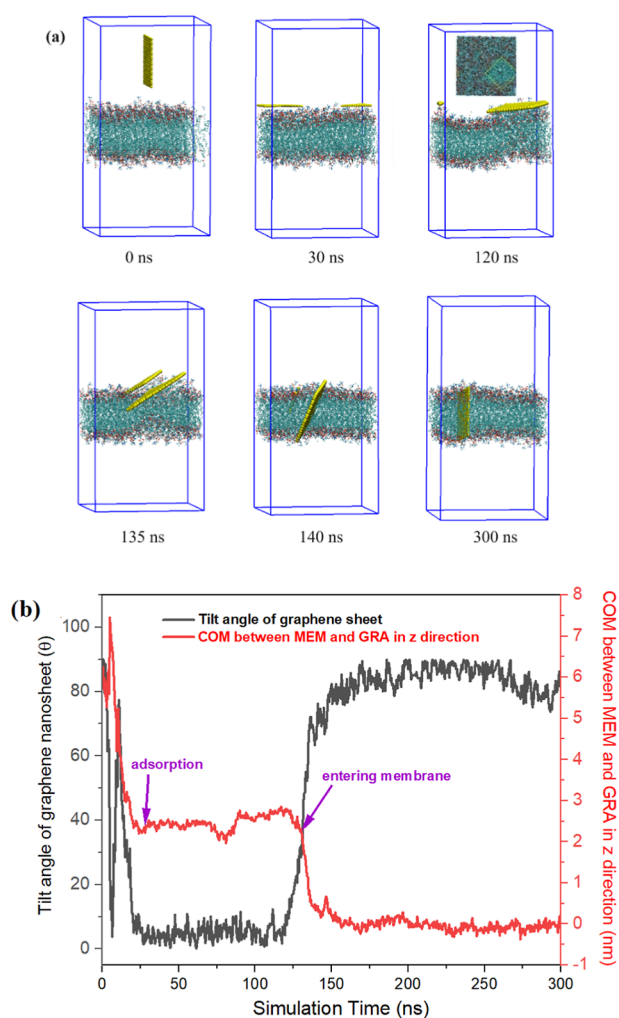


**Figure 2.** (a) Snapshots of dynamic interactions between a  $4 \times 4$  nm graphene nanosheet and a DPPC membrane without cholesterol. (b) Evolution of the tilt angle of the graphene nanosheet and the corresponding COM between the graphene nanosheet and DPPC membrane (MEM) during the interaction process.

center of mass (COM) between the graphene nanosheet and DPPC membrane in the  $z$  direction during the interaction process. The tilt angle is defined as the angle between the plane of the graphene nanosheet and the plane of the DPPC membrane. At first, the graphene nanosheet was vertically placed above the DPPC membrane, as shown in Figure 2a at 0 ns (the tilt angle is  $90^\circ$ ). Combining Figure 2a,b, we can see that the graphene nanosheet migrated and rotated randomly in an aqueous environment before coming into contact with the DPPC membrane. Once in contact, the graphene nanosheet was quickly adsorbed onto the surface of the DPPC membrane (at about 30 ns with a tilt angle at  $0^\circ$ ). Here, two small graphene nanosheets simultaneously appear on one membrane, as shown in Figure 2a at 30 ns, originating from periodic boundary conditions. The adsorption process lasted for a long time (about 90 ns). At about 120 ns, the graphene nanosheet tend to incline with one corner implanting into the core of the membrane and at last being vertically inserted into the membrane. This implanting process is verified by the tilt angle, which changed from  $0$  to  $90^\circ$ , again combined with the decrease of the COM to 0 between the graphene nanosheet and membrane. This is the same as in the previously studies

where graphene penetration is preferentially started at corners.<sup>40</sup> Once one corner of the graphene nanosheet breaks the surface of the DPPC membrane, the entry process is very fast, and it only takes about 20 ns before totally cutting in the membrane, as shown in Figure 2a from 120 to 140 ns. During the injection process, the graphene nanosheet diffuses simultaneously along the membrane surface and would randomly move out of the simulated box. Two fragmented graphene sheets appear on the cell membrane at the 135 ns, which is also a result of the periodic boundary condition. After totally implanting, the graphene nanosheet maintained a vertical insertion configuration continuously throughout the subsequent simulations with its base plane parallel to the DPPC tails. Supplemental 300 ns animation is given in the Supporting Information. This result is similar to that of pristine graphene interacting with POPC bilayers.<sup>41–43</sup>

The driving force of graphene insertion comes from the attractive interaction between graphene and the hydrophobic lipid acyl chains in the inner region of the membrane. With the cut-in graphene, the intracellular transmission of signals may be affected. This result is in agreement with my other studies where small-sized nanomaterials with a hydrophobic surface prefer to remain in the hydrophobic core of the lipid bilayer once they overcome the surface hydrophilic layer of the cell membrane.<sup>44</sup> Therefore, nanomaterials decorated with different ligands are adopted to realize the transmembrane function and deliver drugs in experiments.<sup>45</sup> In addition, two-dimensional nanomaterials with a large size have shown antibacterial activity, such as graphene oxide and  $\text{MoS}_2$ . The lipid in the cell membrane will be destructively extracted by two-dimensional nanomaterials due to the exceptionally strong dispersion interactions and will ultimately disrupt the integrity of bacterial cells.<sup>46,47</sup> In order to avoid such disruption, small graphene nanosheets are used in this work. But research studies have demonstrated that both the insertion of blade-like graphene nanosheets and the destructive extraction of lipid molecules by the presence of the lipophilic graphene have been proposed to cause death of the bacterial cell.<sup>48</sup>

It has been studied that the dynamic behavior of graphene oxide nanosheets on the phospholipid membrane is significantly affected by the lipid phase, which is mainly influenced by the compositions of the cell membrane.<sup>52</sup> Cholesterols are ubiquitous in eukaryotic cells and have been verified to influence the fluidity and permeability of the cell membrane. Therefore, the effect of cholesterol on the dynamic interactions between graphene nanosheets and the phospholipid membrane is necessary to be considered. Here, the dynamics interactions between a pristine graphene nanosheet with a size of  $4 \times 4$  nm and a DPPC membrane with 20% cholesterol are simulated with molecular dynamics simulations. Figure 3a shows the snapshots of the interaction process, in which the cholesterol are represented by purple particles with the hydroxyl groups in the head represented by orange and white atoms. Figure 3b shows the corresponding tilt angle of the graphene nanosheet and the distance of the COM between the graphene nanosheet and the DPPC membrane, defined as previously. We can see that the graphene nanosheet takes two stages before stabilization as well: adsorption and implanting. During the first stage, the graphene nanosheet rotates from an upright state to a horizontal state as it descends to the surface of the bilayer, which is the same as that on a pure DPPC membrane. After adsorption proceeds for a while (at about 60 ns), the graphene

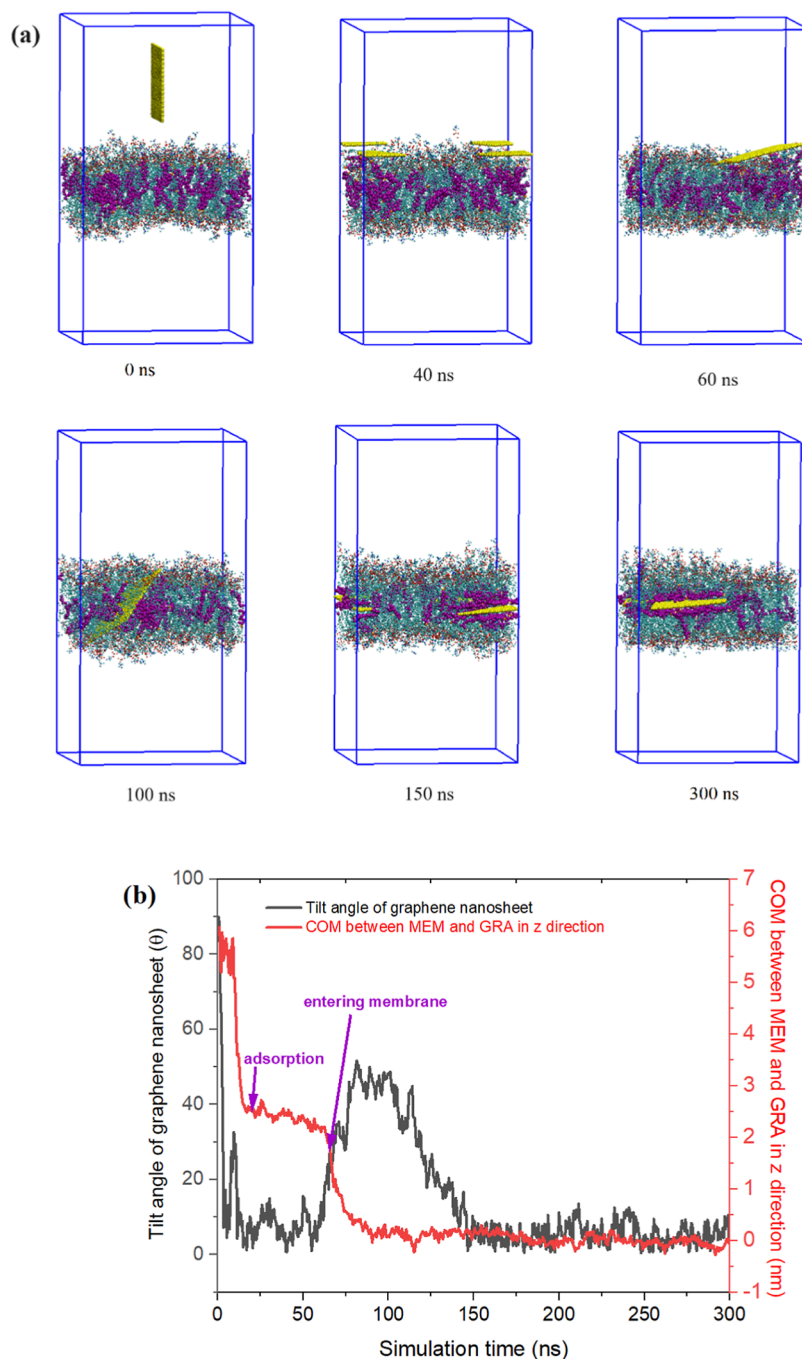


**Figure 3.** (a) Dynamic interactions between a 4 × 4 nm graphene nanosheet and a DPPC membrane with 20% cholesterol. (b) Evolution of the tilt angle of the graphene nanosheet and the corresponding COM between the graphene nanosheet and DPPC membrane during the interaction process.

nanosheet begins to incline and starts to implant into the membrane from one corner. Interestingly, after almost insertion, as shown in Figure 3b at about 100 ns, the graphene nanosheet begins to lie down again and slides to the middle of the two DPPC leaflets horizontally to form a sandwiched superstructure (as shown at 150 ns in Figure 3a). The multifragmented graphene nanosheets in one simulation box are a result of the periodic boundary condition. Similar superstructures have been obtained in POPC bilayers, in which a graphene sheet is buried in a micelle that is covered by POPC lipids.<sup>51</sup> Both theoretical and experimental studies have demonstrated that the hybrid superstructure is mechanically

stable and the natural lipid bilayer structure will rarely be disturbed by the graphene nanosheet.<sup>50</sup> In our study, this superstructure is stabilized during the entire subsequent simulations (the animation of the supplementary 300 ns is given in the Supporting Information). The intramembrane transport of two-dimensional nanomaterials provides beneficial medical applications for sensing, transport, and biological programming.

Here, it must be noted that when the graphene nanosheet happened to collide vertically with the DPPC membrane while migrating and rotating randomly in aqueous environments, the graphene nanosheet will directly cut into the bilayer without

adsorption on the membrane surface. In that case, graphene nanosheets will eventually be vertically inserted into the cell membrane, unaffected by the cholesterol. Therefore, that case is omitted in the following discussion.

The lipid–graphene–lipid superstructure is relatively rare in simulation studies compared to the cut-in state, but it has indeed been obtained experimentally.<sup>49</sup> Arjmandi-Tash et al. produced a lipid–graphene–lipid assembly by combining the Langmuir–Blodgett and the Langmuir–Schaefer methods and confirmed that the hybrid superstructure is mechanically stable and that graphene does not disturb the natural lipid bilayer structure.<sup>50</sup> With simulations, Titov et al. observed the sandwiched graphene–membrane superstructures by forming micelles of individual graphene flakes covered by phospholipids interacting with the POPC membrane and confirmed that the graphene monolayer can be stabilized in the hydrophobic interior of the bilayer membrane at room temperature.<sup>51</sup> It is in agreement with the results obtained by Chen et al. stating that graphene oxide tends to be sandwiched into the liquid–phase bilayer (DOPC membrane at room temperature due to the unsaturated lipids) but forms a vertical configuration in the gel–phase bilayer (DPPC membrane at room temperature).<sup>52</sup> These studies indicated that the sandwiched structure is a product of a large disturbance of the top lipid layer, while the graphene merges with the membrane. That is why graphene oxide was always used to prepare a sandwiched graphene membrane in experiments. In addition, the sandwiched graphene membrane superstructure has nontrivial effects on membrane properties including roughness, rigidity, and fluidity, and the transport of the graphene oxides sandwiched inside the cell membrane varies from Brownian to Lévy and even directional dynamics. Such sandwiched graphene has applicability in enhancing the efficiency of membrane-specific drug delivery.<sup>53</sup>

Studies have demonstrated that the rigid steroid ring structure of cholesterol in the membrane restricts the motion of other lipid tails and decreases the membrane fluidity and flexibility.<sup>10,11</sup> Based on the above results, a graphene nanosheet, which is similar to a graphene oxide nanosheet, may follow the same regularity. That is to say, the graphene nanosheet would be more inclined to vertically insert into the membrane with cholesterol, with which the membrane fluidity has decreased. These views are exactly the opposite of our findings. Therefore, the internal factors that affect the dynamic interactions between the graphene nanosheet and cell membrane have to be further investigated.

The relationship between the mode of entry of graphene into cell membranes, graphene size, and cholesterol concentration was systematically investigated. Three graphene nanosheets with sizes of  $3 \times 3$ ,  $4 \times 4$ , and  $5 \times 5$  nm are tested, and the mole percentages of cholesterol are 0, 10, 20, and 30%. The simulation results are represented by the phase diagram in Figure 4. We found that the mole percentage of cholesterol in the DPPC membrane is the key factor affecting the final state of the graphene nanosheet. As cholesterol percentage increases, the graphene nanosheet gradually changes from a cut-in configuration to a sandwiched superstructure, which is independent of the size of the graphene nanosheet. In addition, the critical mole percentage of cholesterol for a graphene nanosheet to change its configuration is nanosheet size-dependent. When the mole percentage of cholesterol reaches 30%, graphene nanosheets are always sandwiched in the middle of the DPPC bilayers.

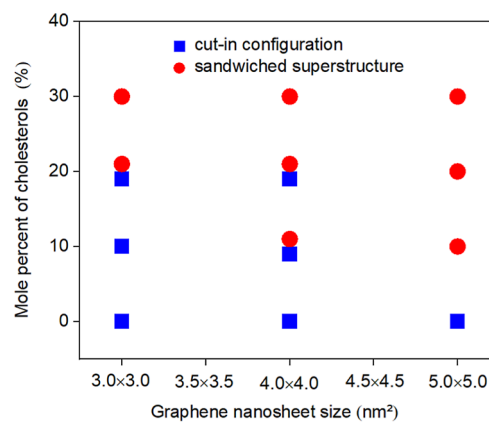


**Figure 4.** Phase diagram of the final configurations of graphene nanosheets with different sizes and the DPPC membrane containing different mole percentages of cholesterol.

The larger the size of graphene nanosheets, the less the amount of cholesterol required to change the final configuration. Only 10% cholesterol are needed for the graphene nanosheet with a size of  $5 \times 5$  nm to become a sandwiched superstructure. At a certain cholesterol concentration, both configurations will occur, such as  $4 \times 4$  nm graphene nanosheets with DPPC membranes containing 10 and 20% cholesterol. Figure 4 illustrates that the final configurations of the graphene nanosheet in the DPPC membrane is not only related to the mole percentage of cholesterol but also related to the size of the graphene nanosheet.

To explore the reasons for the different configurations of the graphene nanosheet caused by cholesterol, the dynamic process between cholesterol and the graphene nanosheet was studied. Figure 5 gives the density distribution evolution of cholesterol in the DPPC membrane (upper row) and carbon atoms in the graphene nanosheet (down row) during the adsorption process in Figure 3, in which the size of the graphene nanosheet is  $4 \times 4$  nm and the mole percentage of cholesterol is 20%. The densities are separately counted in three stages with a time interval of 10 ns in each. The three stages are the initial stage (0–10 ns), adsorption for a while (25–35 ns), and before implantation into the membrane (50–60 ns), respectively. We can see that after adsorption of the graphene nanosheet on the surface of the DPPC membrane, the location of the cholesterol and graphene nanosheet is gradually synchronized over time. It means that during the adsorption of the graphene nanosheet, the cholesterol in the DPPC membrane are inclined to aggregate beneath the graphene nanosheet, or the graphene nanosheet is inclined to move to the areas with more cholesterol. This may be due to the stronger dispersion interactions between cholesterol and the graphene nanosheet than with DPPC lipids. Studies have shown that cholesterol prefer to adhere to the surface of the graphene nanosheet in the cell membrane or in an aqueous environment when they are encountered.<sup>29</sup> Our study shows that the mutual attraction between cholesterol and graphene nanosheets is already effective before they are contacted. Therefore, there is a significant change of local composition in the cell membrane beneath the graphene nanosheet.

In order to explore the interference of the graphene nanosheet with the order of the cell membrane during the interaction process, the inclination angles of DPPC tails in cholesterol-containing and cholesterol-free cell membranes

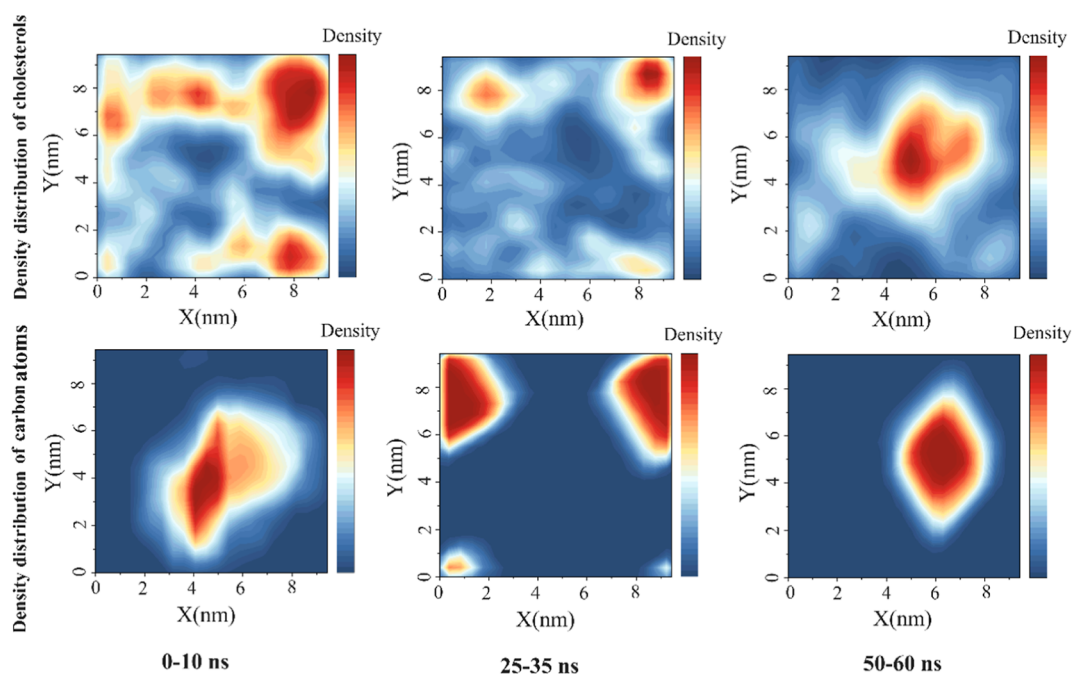


**Figure 5.** Density distribution evolution of cholesterols and that of carbon atoms in the graphene nanosheet before the graphene nanosheet is implanted into the DPPC membrane.

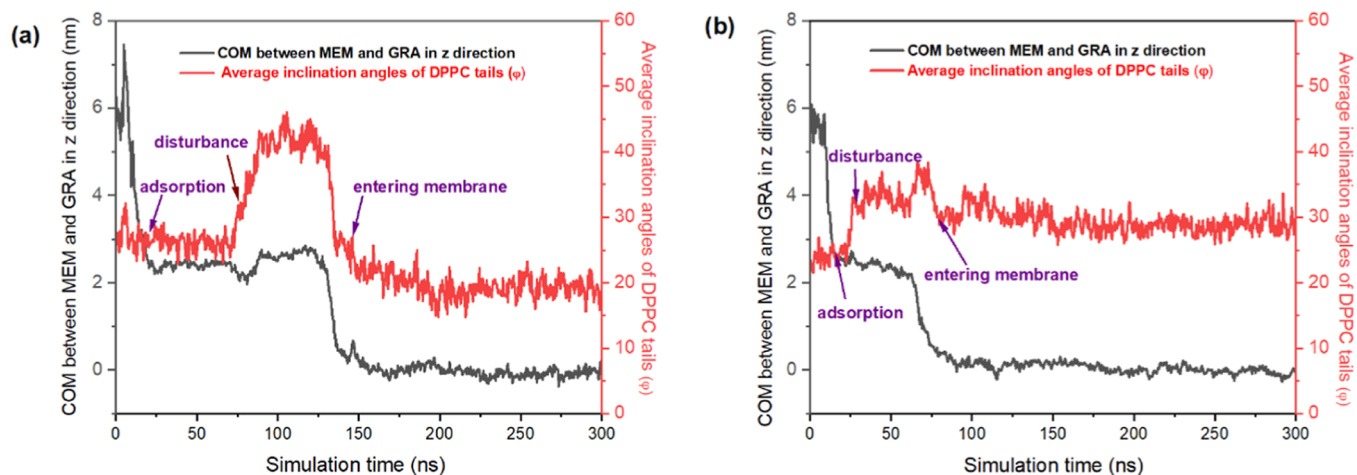


**Figure 6.** Averaged inclination angles of DPPC tails near graphene nanosheet and the corresponding COM between the graphene nanosheet and DPPC membrane. (a) The case of a 4 nm × 4 nm graphene nanosheet interacting with a pure DPPC membrane in Figure 2. (b) The case of a 4 × 4 nm graphene nanosheet interacting with a DPPC membrane containing 20% cholesterols in Figure 3.

were calculated, respectively. Figure 6 shows the average inclination angle of the DPPC tails within the 1 nm range around the graphene nanosheet as well as the corresponding COM between the graphene nanosheet and DPPC membrane in  $z$  direction during the entering process of the graphene nanosheet. The inclination angle  $\varphi$  is defined as the angle between the normal vector of the membrane and the vector from the last carbon atom in each DPPC tail to the ester group that connects the two tails. Therefore, the larger the averaged inclination angle of DPPC tails, the greater the interference of graphene with DPPC lipids.

Figure 6a shows that the pure DPPC lipids in the membrane were affected after a short period of adsorption of the graphene nanosheet. With the adsorption of the graphene nanosheet on the membrane surface, the tails of DPPC lipids beneath the graphene nanosheet start to jump out of the bilayer and adhere

to the lower surface of the graphene nanosheet, which seriously affects the orientation of the lipid tails, as shown with magnification in Figure 2a at 120 ns. Thus, the inclination angles of DPPC tails have a large increase. With the insertion of the graphene nanosheet into the DPPC membrane from one corner (at about 140 ns in Figure 2a), the locally disturbed DPPC reassembled to a regular bilayer structure synchronously and the inclination angles of the DPPC tails recovered to the original state quickly. Upon a closer observation, we found that after the insertion of the graphene nanosheet, the averaged inclination angles of the DPPC tails become even smaller than in the initial state, which means that the graphene nanosheet with a cut-in state makes the local membrane more regular. Although the packing state of lipids has been greatly changed, transmembrane leakage is not observed during that process in our simulations. This should be attributed to dispersion

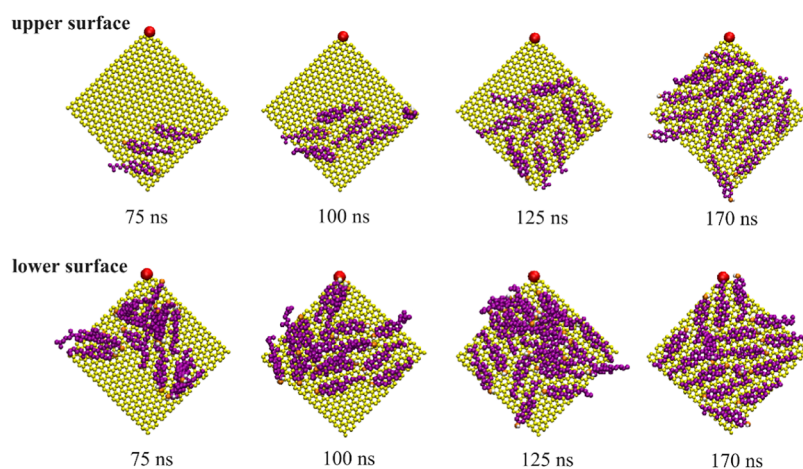


**Figure 7.** Snapshots of the adsorption of cholesterols on both sides of the graphene nanosheet during the implanting process.

interactions of graphene and DPPC tails, as well as the structural matching between the regular two-dimensional structure of graphene and the saturated double chain tails of DPPC in the bilayer state.

Figure 6b is the evolution of the averaged inclination angles of DPPC tails during the entering of a  $4 \times 4$  nm graphene nanosheet into a DPPC membrane with 20% cholesterols. Due to the facts that cholesterols are more easily adsorbed on the surface of graphene than on the DPPC tails, graphene nanosheets on the surface of cell membranes are more likely to extract some cholesterols. In that case, the amount of DPPC tails adsorbed on the lower surface of graphene is smaller than that in a pure DPPC membrane, which makes graphene less disruptive to the cell membrane containing cholesterols. With the implanting of the graphene nanosheet, the averaged inclination angle of DPPC tails changes from about  $35$  to  $30^\circ$  and is continuously maintained at that degree, which is still larger than that when undisturbed (averaged inclination angle at  $25^\circ$ ). This may be due to the continuous adsorption of cholesterols on the surface of graphene. Compared to that in the pure DPPC membrane, the DPPC tails cannot adsorb regularly to the uneven surface of graphene-adsorbed cholesterols. Instead, they can only partially be adsorbed on cholesterols and partially be adsorbed on the surface of graphene. Therefore, the averaged inclination of the DPPC tails must be larger than that without cholesterols. That is to say, cholesterols adsorbed on the surface of graphene reduce the order of DPPC tails during the implanting process, together with graphene, instead of increasing the orderliness of the DPPC tail in a stable cell membrane.

To further analyze the effect of cholesterols on the implanting process of graphene nanosheets more clearly, the behavior of cholesterols near graphene nanosheets is investigated. Figure 7 gives the snapshots of the adsorption of cholesterols on the upper surface (top row) and lower surface (bottom row) of the graphene nanosheet during its rotation from an inclined cut-in state to a sandwiched state, as shown in Figure 3. To see the adsorbed cholesterols more clearly, we observed it from the upper and lower surfaces of the graphene nanosheet, respectively. The red dot represents the last carbon atom to enter the DPPC membrane. It shows that the cholesterols are first adsorbed on the lower surface of the graphene nanosheet. During the implanting process of graphene into the DPPC bilayer, the surrounding cholesterols continuously adsorb onto the lower surface of graphene, while

some quickly adsorb onto the upper surface of graphene. Cooperative reorientation of cholesterols on the graphene surface was observed to maximize hydrophobic interactions with the graphene surface. The adsorption of cholesterols on both sides of the graphene nanosheet further perturbs the DPPC tails, which makes it difficult to see a decrease of the average inclination angle of DPPC tails during the implanting process. That is to say, the increase in the local disturbance of the DPPC tails is a result of adsorption of cholesterols along the surface of graphene, and the low order of DPPC tails results in graphene adopting a sandwiched configuration. It coincides with the mechanism proposed in ref 52.

As for the membrane model composed of DOPC and POPC, whose tails are unsaturated, the order of the membrane is naturally lower than that with DPPC lipids. In that case, a sandwiched graphene-membrane may be obtained by a small additional disturbance, such as lower cholesterol concentration, partially oxidized graphene, and even other geometrically mismatched molecules. Based on this analysis, it is not difficult for us to discover that in the experiment, graphene oxide nanosheets are usually used to prepare the sandwiched graphene-cell membrane superstructure rather than the pristine graphene nanosheet.<sup>53</sup>

Figure 8 gives the angular distribution of the 20% cholesterols before the adsorption of the  $4 \times 4$  nm graphene nanosheet and after the final adsorption of the graphene nanosheet with a sandwiched configuration. The angle  $\beta$  is defined as the angle between the cholesterol molecular orientation and the normal direction of the cell membrane. It shows that without the graphene nanosheet, cholesterols prefer to mix with phospholipid molecules in an upright state ( $\beta$  tends to  $15^\circ$ ). After the implanting of the graphene nanosheet with a sandwiched structure, the cholesterols are divided into two states, adsorbed horizontally on the surface of the graphene nanosheet ( $\beta$  tends to  $90^\circ$ ) and standing upright freely ( $\beta$  tends to  $15^\circ$ ) in the DPPC membrane. The inset in Figure 8 is the magnified configuration of the sandwiched structure. It shows that the thickness of the cell membrane at the sandwiched structure exhibits an increase.

Based on the above discussion, cholesterols are important factors that influence the dynamic interactions between the graphene nanosheet and the DPPC membrane. To verify the reason for obtaining different final configurations with the same cholesterol concentration, such as  $4 \text{ nm} \times 4 \text{ nm}$  graphene nanosheet entering the cell membrane containing 20%

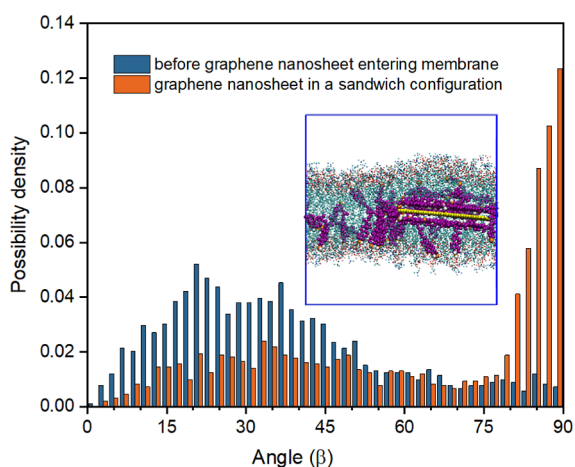


**Figure 8.** Angular distribution of cholesterols before the graphene nanosheet enters the membrane and after graphene forms a sandwiched structure with the cell membrane. The insertion is a snapshot of cholesterols and the graphene nanosheet with a sandwiched configuration.

cholesterol, the amount of cholesterols on the surface of the nanographene nanosheet during the implanting processes in the two cases are calculated, as shown in Figure 9. The tilt angles of graphene nanosheets in both cases are provided to distinguish these two processes and the final structure. We can see that the number of cholesterols adsorbed on the graphene nanosheet with the final cut-in state (in Figure 9a) is much less than that on the final sandwiched state (in Figure 9b). This result further indicates that the adsorption amount of cholesterols on the surface of the graphene nanosheet is the key factor affecting the final state of the graphene nanosheet.

Combined with the results in Figure 6, we can see that the amount of adsorbed cholesterol affects the order of the DPPC tails and ultimately affects the state of the graphene nanosheet in the cell membrane. Therefore, the graphene nanosheet is prone to form sandwich structures in cell membranes with high cholesterol percentage as high percentages of cholesterols are more suitable for adsorption onto the graphene nanosheet. Meanwhile, a low cholesterol percentage is required for a large graphene nanosheet to become a sandwiched superstructure.

Because cholesterols are easier to accumulate on large surfaces of graphene. In the phase diagram in Figure 4, we can see that only 10% cholesterols are needed for the graphene nanosheet with a size of 5 nm × 5 nm to become a sandwiched superstructure. Furthermore, a large graphene nanosheet is inherently inclined to be hosted in the hydrophobic interior of biological membranes and form a sandwich superstructure to achieve maximized hydrophobic interactions. In the following, properties of the cell membrane with the graphene nanosheet sandwiched in the core of bilayers will be investigated in details.

So far, much effort has been invested in exploring the functions of nanomaterials and the potential harm for their applications in biomedical engineering. Nanoparticles with different properties and two-dimensional flakes, such as graphene, boron nitride, and black phosphorus nanosheets, are research hot spots. Due to the complexity, attention is paid to the mutual interactions between nanomaterials and the cell membrane with different lipids. In fact, membrane proteins and cholesterols that are much different from the amphiphilic lipids may have a greater impact on their interactions, such as the phenomenon in this work.

In summary, in this paper, the effect of cholesterols on the dynamic interactions between the graphene nanosheet and DPPC membrane is studied using molecular dynamics simulations. It showed that due to preferential adsorptions between cholesterols and the graphene nanosheet, cholesterols are swiftly adsorbed onto the surface of the graphene nanosheet once it enters the DPPC membrane. The adsorbed cholesterols disturb the local order of the DPPC membrane and transform it from a gel-like phase to a liquid-like phase. Therefore, the graphene nanosheet is inclined to form a sandwiched superstructure in the cell membrane with enough cholesterols. It is opposite to our ordinary cognition that cholesterols increase the order and rigidity of the cell membrane and maintain the cell membrane integrity. Our studies elucidate that in studying the transport capacity or toxicity of nanomaterials, cholesterols are an essential factor that cannot be ignored, and they may provide some explanations for conflicts between experiments and theoretical studies. With the sandwiched superstructures, graphene

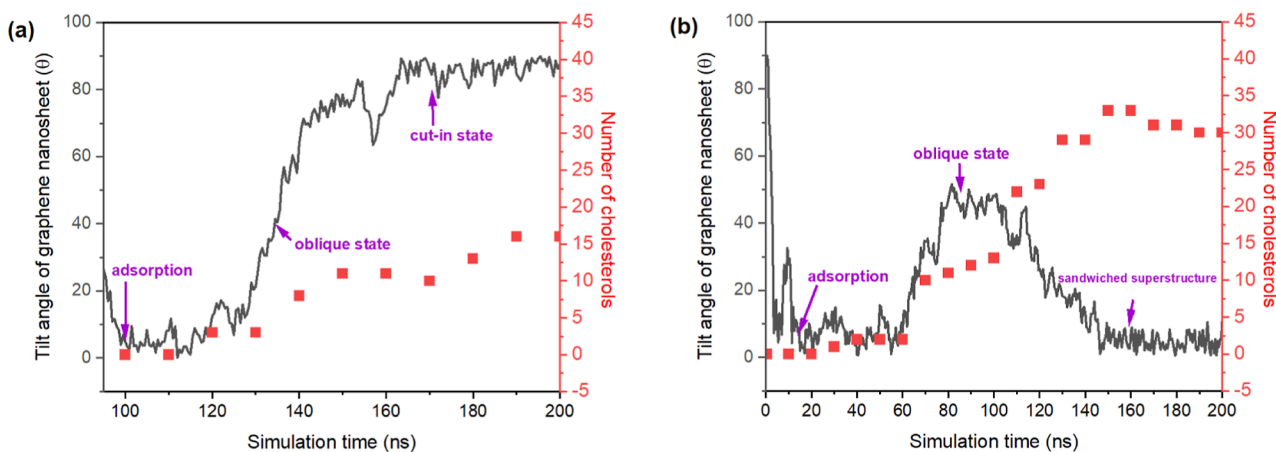


**Figure 9.** Tilt angle of a 4 × 4 nm graphene sheet and the corresponding adsorbed number of cholesterols during two different modes of implanting. (a) Graphene nanosheet ultimately in the cell membrane with a cut-in state. (b) Graphene nanosheet ultimately forming a sandwiched state in the cell membrane.

nanosheets may be useful in intracellular signal transmission and drug delivery.

## ■ ASSOCIATED CONTENT

### SI Supporting Information

The Supporting Information is available free of charge at <https://pubs.acs.org/doi/10.1021/acsomega.3c08236>.

Animation of the upright stable state (MP4)

Animation of the sandwiched stable state (MP4)

## ■ AUTHOR INFORMATION

### Corresponding Authors

**Juanmei Hu** – Key Laboratory of Optical Field Manipulation of Zhejiang Province, Department of Physics, Zhejiang Sci-Tech University, Hangzhou 310018, China; [orcid.org/0000-0003-1287-1260](https://orcid.org/0000-0003-1287-1260); Email: [hjm@zstu.edu.cn](mailto:hjm@zstu.edu.cn)

**Fengmin Wu** – Key Laboratory of Optical Field Manipulation of Zhejiang Province, Department of Physics, Zhejiang Sci-Tech University, Hangzhou 310018, China; Email: [wfm@zstu.edu.cn](mailto:wfm@zstu.edu.cn)

### Author

**Binbin Tan** – Key Laboratory of Optical Field Manipulation of Zhejiang Province, Department of Physics, Zhejiang Sci-Tech University, Hangzhou 310018, China

Complete contact information is available at:

<https://pubs.acs.org/doi/10.1021/acsomega.3c08236>

### Notes

The authors declare no competing financial interest.

## ■ ACKNOWLEDGMENTS

This work was supported by the Natural Science Foundation of Zhejiang Province (no. LTY22F020002).

## ■ REFERENCES

- (1) Abbasi Kajani, A.; Haghjooy Javanmard, S.; Asadnia, M.; Razmjou, A. Recent Advances in Nanomaterials Development for Nanomedicine and Cancer. *ACS Appl. Bio Mater.* **2021**, *4*, 5908–5925.
- (2) Bauri, S.; Tripathi, S.; Choudhury, A. M.; Mandal, S. S.; Raj, H.; Maiti, P. Nanomaterials as Theranostic Agents for Cancer Therapy. *ACS Appl. Nano Mater.* **2023**, *6*, 21462–21495.
- (3) Tripathi, A.; Bonilla-Cruz, J. Review on Health care Biosensing Nanomaterials. *ACS Appl. Nano Mater.* **2023**, *6*, 5042–5074.
- (4) Cai, P.; Zhang, X.; Wang, M.; Wu, Y.; Chen, X. Combinatorial Nano-Bio Interfaces. *ACS Nano* **2018**, *12*, 5078–5084.
- (5) Cebeacuer, M.; Amaro, M.; Jurkiewicz, P.; Sarmento, M. J.; Sachl, R.; Cwiklik, L.; Hof, M. Membrane Lipid Nanodomains. *Chem. Rev.* **2018**, *118*, 11259–11297.
- (6) Li, Z.; Zhang, Y.; Chan, C.; Zhi, C.; Cheng, X.; Fan, J. Temperature-Dependent Lipid Extraction from Membranes by Boron Nitride Nanosheets. *ACS Nano* **2018**, *12*, 2764–2772.
- (7) Jiang, D.; Devadoss, A.; Palencsár, M. S.; Fang, D.; White, N. M.; Kelley, T. J.; Smith, J. D.; Burgess, J. D. Direct Electrochemical Evaluation of Plasma Membrane Cholesterol in Live Mammalian Cells. *J. Am. Chem. Soc.* **2007**, *129*, 11352–11353.
- (8) Havlikova, M.; Szabova, J.; Mravcova, L.; Venerova, T.; Chang, C. H.; Pekar, M.; Jugl, A.; Mravec, F. Cholesterol Effect on Membrane Properties of Cationic Ion Pair Amphiphile Vesicles at Different Temperatures. *Langmuir* **2021**, *37* (7), 2436–2444.
- (9) Ohvo-Rekila, H.; Ramstedt, B.; Leppimäki, P.; Slotte, J. P. Cholesterol interactions with phospholipids in membranes. *Prog. Lipid Res.* **2002**, *41*, 66–97.
- (10) Jeon, J. H.; Monne, H. M.; Javanainen, M.; Metzler, R. Anomalous diffusion of phospholipids and cholesterol in a lipid bilayer and its origins. *Phys. Rev. Lett.* **2012**, *109* (18), 188103.
- (11) Regmi, R.; Winkler, P. M.; Flauraud, V.; Borgman, K. J. E.; Manzo, C.; Brugger, J.; Rigneault, H.; Wenger, J.; Garcia-Parajo, M. F. Planar Optical Nanoantennas Resolve Cholesterol-Dependent Nanoscale Heterogeneities in the Plasma Membrane of Living Cells. *Nano Lett.* **2017**, *17* (10), 6295–6302.
- (12) Smondryev, A. M.; Berkowitz, M. L. Structure of Dipalmitoylphosphatidylcholine/Cholesterol Bilayer at Low and High Cholesterol Concentrations: Molecular Dynamics Simulation. *Biophys. J.* **1999**, *77*, 2075–2089.
- (13) Nagle, J. F. Measuring the bending modulus of lipid bilayers with cholesterol. *Phys. Rev. E* **2021**, *104* (4), 044405.
- (14) Rog, T.; Pasenkiewicz-Gierula, M.; Vattulainen, I.; Karttunen, M. Ordering effects of cholesterol and its analogues. *Biochim. Biophys. Acta* **2009**, *1788* (1), 97–121.
- (15) Aghaaminiha, M.; Farnoud, A. M.; Sharma, S. Quantitative relationship between cholesterol distribution and ordering of lipids in asymmetric lipid bilayers. *Soft Matter* **2021**, *17* (10), 2742–2752.
- (16) Elkins, M. R.; Sergeev, I. V.; Hong, M. Determining Cholesterol Binding to Membrane Proteins by Cholesterol (13)C Labeling in Yeast and Dynamic Nuclear Polarization NMR. *J. Am. Chem. Soc.* **2018**, *140* (45), 15437–15449.
- (17) Milogrodzka, L.; Nguyen Pham, D. T.; Sama, G. R.; Samadian, H.; Zhai, J.; de Campo, L.; Kirby, N. M.; Scott, T. F.; Banaszak Holl, M. M.; vant Hag, L. Effect of Cholesterol on Biomimetic Membrane Curvature and Coronavirus Fusion Peptide Encapsulation. *ACS Nano* **2023**, *17* (9), 8598–8612.
- (18) Canepa, E.; Bochicchio, D.; Gasbarri, M.; Odino, D.; Canale, C.; Ferrando, R.; Canepa, F.; Stellacci, F.; Rossi, G.; Dante, S.; Relini, A. Cholesterol Hinders the Passive Uptake of Amphiphilic Nanoparticles into Fluid Lipid Membranes. *J. Phys. Chem. Lett.* **2021**, *12* (35), 8583–8590.
- (19) Hu, Y.; Patel, S. Thermodynamics of cell-penetrating HIV1 TAT peptide insertion into PC/PS/CHOL model bilayers through transmembrane pores: the roles of cholesterol and anionic lipids. *Soft Matter* **2016**, *12* (32), 6716–6727.
- (20) Lorents, A.; Saalik, P.; Langel, U.; Pooga, M. Arginine-Rich Cell-Penetrating Peptides Require Nucleolin and Cholesterol-Poor Subdomains for Translocation across Membranes. *Bioconjugate Chem.* **2018**, *29* (4), 1168–1177.
- (21) Zhang, L.; Bennett, W. F.; Zheng, T.; Ouyang, P. K.; Ouyang, X.; Qiu, X.; Luo, A.; Karttunen, M.; Chen, P. Effect of Cholesterol on Cellular Uptake of Cancer Drugs Pirarubicin and Ellipticine. *J. Phys. Chem. B* **2016**, *120* (12), 3148–3156.
- (22) Wang, X. D.; Kim, C.; Zhang, Y.; Rindhe, S.; Cobb, M. H.; Yu, Y. Cholesterol Regulates the Tumor Adaptive Resistance to MAPK Pathway Inhibition. *J. Proteome Res.* **2021**, *20* (12), 5379–5391.
- (23) Iannazzo, D.; Pistone, A.; Salamò, M.; Galvagno, S.; Romeo, R.; Giofrè, S. V.; Branca, C.; Visalli, G.; Di Pietro, A. Graphene quantum dots for cancer targeted drug delivery. *Int. J. Pharm.* **2017**, *518* (1–2), 185–192.
- (24) Xue, Z.; Sun, Q.; Zhang, L.; Kang, Z.; Liang, L.; Wang, Q.; Shen, J. W. Graphene quantum dot assisted translocation of drugs into a cell membrane. *Nanoscale* **2019**, *11* (10), 4503–4514.
- (25) Rahimi, S.; Chen, Y.; Zareian, M.; Pandit, S.; Mijakovic, I. Cellular and subcellular interactions of graphene-based materials with cancerous and non-cancerous cells. *Adv. Drug Delivery Rev.* **2022**, *189*, 114467.
- (26) Mandal, P.; Ghosh, S. K. Graphene-Based Nanomaterials and Their Interactions with Lipid Membranes. *Langmuir* **2023**, *39* (51), 18713–18729.
- (27) Hu, X.; Zhou, Q. Health and ecosystem risks of graphene. *Chem. Rev.* **2013**, *113* (5), 3815–3835.
- (28) Bernabo, N.; Machado-Simoes, J.; Valbonetti, L.; Ramal-Sanchez, M.; Capacchietti, G.; Fontana, A.; Zappacosta, R.; Palestini, P.; Botto, L.; Marchisio, M.; Lanuti, P.; Ciulla, M.; Di Stefano, A.; Fioroni, E.; Spina, M.; Barboni, B. Graphene Oxide increases

- mammalian spermatozoa fertilizing ability by extracting cholesterol from their membranes and promoting capacitation. *Sci. Rep.* **2019**, *9* (1), 8155.
- (29) Zhang, L.; Wang, X. Mechanisms of graphyne-enabled cholesterol extraction from protein clusters. *RSC Adv.* **2015**, *5* (16), 11776–11785.
- (30) Kang, I.; Yoo, J. M.; Kim, D.; Kim, J.; Cho, M. K.; Lee, S. E.; Kim, D. J.; Lee, B. C.; Lee, J. Y.; Kim, J. J.; Shin, N.; Choi, S. W.; Lee, Y. H.; Ko, H. S.; Shin, S.; Hong, B. H.; Kang, K. S. Graphene Quantum Dots Alleviate Impaired Functions in Niemann-Pick Disease Type C in Vivo. *Nano Lett.* **2021**, *21* (5), 2339–2346.
- (31) Kitko, K. E.; Hong, T.; Lazarenko, R. M.; Ying, D.; Xu, Y.-Q.; Zhang, Q. Membrane cholesterol mediates the cellular effects of monolayer graphene substrates. *Nat. Commun.* **2018**, *9* (1), 796.
- (32) Kukol, A. Lipid Models for United-Atom Molecular Dynamics Simulations of Proteins. *J. Chem. Theory Comput.* **2009**, *5* (3), 615–626.
- (33) Berger, O.; Edholm, O.; Jähnig, F. Molecular dynamics simulations of a fluid bilayer of dipalmitoylphosphatidylcholine at full hydration, constant pressure, and constant temperature. Constant Pressure, and Constant Temperature. *Biophys. J.* **1997**, *72*, 2002–2013.
- (34) Schmid, N.; Eichenberger, A. P.; Choutko, A.; Riniker, S.; Winger, M.; Mark, A. E.; van Gunsteren, W. F. Definition and testing of the GROMOS force-field versions 54A7 and 54B7. *Eur. Biophys. J.* **2011**, *40* (7), 843–856.
- (35) Patra, N.; Wang, B.; Král, P. Nanodroplet Activated and Guided Folding of Graphene Nanostructures. *Nano Lett.* **2009**, *9* (11), 3766–3771.
- (36) Hummer, G.; Rasaiah, J. C.; Noworyta, J. P. water conduction through the hydrophobic channel of a carbon nanotube. *Nature* **2001**, *414* (6860), 188–190.
- (37) Berendsen, H. J. C.; Postma, J. P. M.; Gunsteren, W. F. v.; Hermans, J. Interaction models for water in relation to protein hydration. *Intermolecular Forces*; Springer, 1981; pp 331–342.
- (38) Venable, R. M. C.; Chen, L. E.; Pastor, R. W. Comparison of the Extended Isotropic Periodic Sum and Particle Mesh Ewald Methods for Simulations of Lipid Bilayers and Monolayers. *J. Phys. Chem. B* **2009**, *113*, 5855–5862.
- (39) Liu, C.; Elvati, P.; Majumder, S.; Wang, Y.; Liu, A. P.; Violi, A. Predicting the Time of Entry of Nanoparticles in Lipid Membranes. *ACS Nano* **2019**, *13* (9), 10221–10232.
- (40) Li, Y.; Yuan, H.; von dem Bussche, A.; Creighton, M.; Hurt, R. H.; Kane, A. B.; Gao, H. Graphene microsheets enter cells through spontaneous membrane penetration at edge asperities and corner sites. *Proc. Natl. Acad. Sci. U.S.A.* **2013**, *110* (30), 12295–12300.
- (41) Kong, Z.; Zhang, P.; Chen, J.; Zhou, H.; Ma, X.; Wang, H.; Shen, J. W.; Liang, L. J. Effect of Shape on the Entering of Graphene Quantum Dots into a Membrane: A Molecular Dynamics Simulation. *ACS Omega* **2021**, *6* (16), 10936–10943.
- (42) Chen, J.; Zhou, G.; Chen, L.; Wang, Y.; Wang, X.; Zeng, S. Interaction of Graphene and its Oxide with Lipid Membrane: A Molecular Dynamics Simulation Study. *J. Phys. Chem. C* **2016**, *120* (11), 6225–6231.
- (43) Liang, L.; Kong, Z.; Kang, Z.; Wang, H.; Zhang, L.; Shen, J. W. Theoretical Evaluation on Potential Cytotoxicity of Graphene Quantum Dots. *ACS Biomater. Sci. Eng.* **2016**, *2* (11), 1983–1991.
- (44) Gupta, R.; Badhe, Y.; Mitragotri, S.; Rai, B. Permeation of nanoparticles across the intestinal lipid membrane: dependence on shape and surface chemistry studied through molecular simulations. *Nanoscale* **2020**, *12* (11), 6318–6333.
- (45) Lin, X.; Lin, X.; Gu, N. Optimization of hydrophobic nanoparticles to better target lipid rafts with molecular dynamics simulations. *Nanoscale* **2020**, *12* (6), 4101–4109.
- (46) Tu, Y.; Lv, M.; Xiu, P.; Huynh, T.; Zhang, M.; Castelli, M.; Liu, Z.; Huang, Q.; Fan, C.; Fang, H.; Zhou, R. Destructive extraction of phospholipids from *Escherichia coli* membranes by graphene nanosheets. *Nat. Nanotechnol.* **2013**, *8* (8), 594–601.
- (47) Kumari, M.; Kashyap, H. K. Wrapping-Trapping versus Extraction Mechanism of Bactericidal Activity of MoS<sub>2</sub> Nanosheets against *Staphylococcus aureus* Bacterial Membrane. *Langmuir* **2023**, *39*, 5440–5453.
- (48) Pham, Vy T. H.; Truong, V. K.; Quinn, M. D. J.; Notley, S. M.; Guo, Y.; Baulin, V. A.; Al Kobaisi, M.; Crawford, R. J.; Ivanova, E. P. Graphene Induces Formation of Pores That Kill Spherical and Rod-Shaped Bacteria. *ACS Nano* **2015**, *9* (8), 8458–8467.
- (49) Mu, C.; Xing, D.; Zhang, D.; Gong, C.; Wang, J.; Zhao, L.; Li, D.; Zhang, X. Mass Spectrometry and Cryogenic Electron Microscopy Illuminate Molecular-Level Mechanisms of the Oxidative and Structural Damage to Lipid Membranes by Radical-Bearing Graphene Oxide. *J. Phys. Chem. Lett.* **2022**, *13* (11), 2638–2643.
- (50) Arjmandi-Tash, H.; Lima, L. M. C.; A Belyaeva, L.; Mukhina, T.; Fragneto, G.; Kros, A.; Charitat, T.; Schneider, G. F. Encapsulation of Graphene in the Hydrophobic Core of a Lipid Bilayer. *Langmuir* **2020**, *36* (48), 14478–14482.
- (51) Titov, A. V.; Král, P.; Pearson, R. Sandwiched Graphene-Membrane Superstructures. *ACS Nano* **2010**, *4* (1), 229–234.
- (52) Chen, Z.; Lu, X.; Liu, J.; Tian, X.; Li, W.; Yang, K.; Yuan, B. Lipid Phase Influences the Dynamic Interactions between Graphene Oxide Nanosheets and a Phospholipid Membrane. *J. Phys. Chem. B* **2021**, *125* (14), 3589–3597.
- (53) Chen, P.; Yue, H.; Zhai, X.; Huang, Z.; Ma, G. H.; Wei, W.; Yan, L. T. Transport of a graphene nanosheet sandwiched inside cell membranes. *Sci. Adv.* **2019**, *5* (6), No. eaaw3192.